Supplementary Materials

Comparison to M-LORAKS reconstruction

We implemented unit tests and compared the output of substeps of PyLORAKS against the latest MLORAKS[1] implementation. Specifically, we focused on achieving equal reconstruction performance under the same settings, when not employing any of the additional features (like randomised matrix decomposition methods). However, there are a number of reasons why the results might only achieve quantitative comparability up to a small numerical variation. First, LORAKS involves matrix decomposition methods, some of which, like the eigenvectors from an eigendecomposition, are not providing a unique solution. Thus, different software and hardware implementations will produce different results. Second, in favor of computational efficiency, we changed the LORAKS matrix operators to be built from squared instead of circular k-space neighbourhood patches, ensuring a similar extent by roughly matching the number of elements. Nonetheless, we tested the comparability of the implementations in a number of settings.

Exemplarily, the joint reconstruction of a test-case, a 3-fold undersampled Shepp-Logan phantom with eight simulated channels and two echoes, is given in Figure 1.

After Fourier transform of the reconstruction, we computed the three metrics (SSIM, NMSE, PSNR) in image space, using the magnitude data of all reconstructed channels and echoes. The values can be seen in Table 1. High agreement between the implementations was achieved.

Table 1: Computed metrics for the validation example showing high agreement between the data reconstructed with MLORAKS and PyLORAKS.

PSNR	NMSE	SSIM
70.745	0.0003	0.9983

SURE parameter optimisation

Stein's unbiased risk estimate can be used in the presence of i.i.d. zero-mean additive Gaussian noise to calculate the expected mean squared error of an estimator. Assume a set of acquired data $\boldsymbol{k}_{\text{acq}} = \boldsymbol{k}_{\text{true}} + \boldsymbol{n} \in \mathcal{C}^m$, where $\boldsymbol{n}$ is the noise with standard deviation σ. We denote $\boldsymbol{P}_\theta \in \mathcal{C}^{m \times m}$ as the symmetric linear operator,

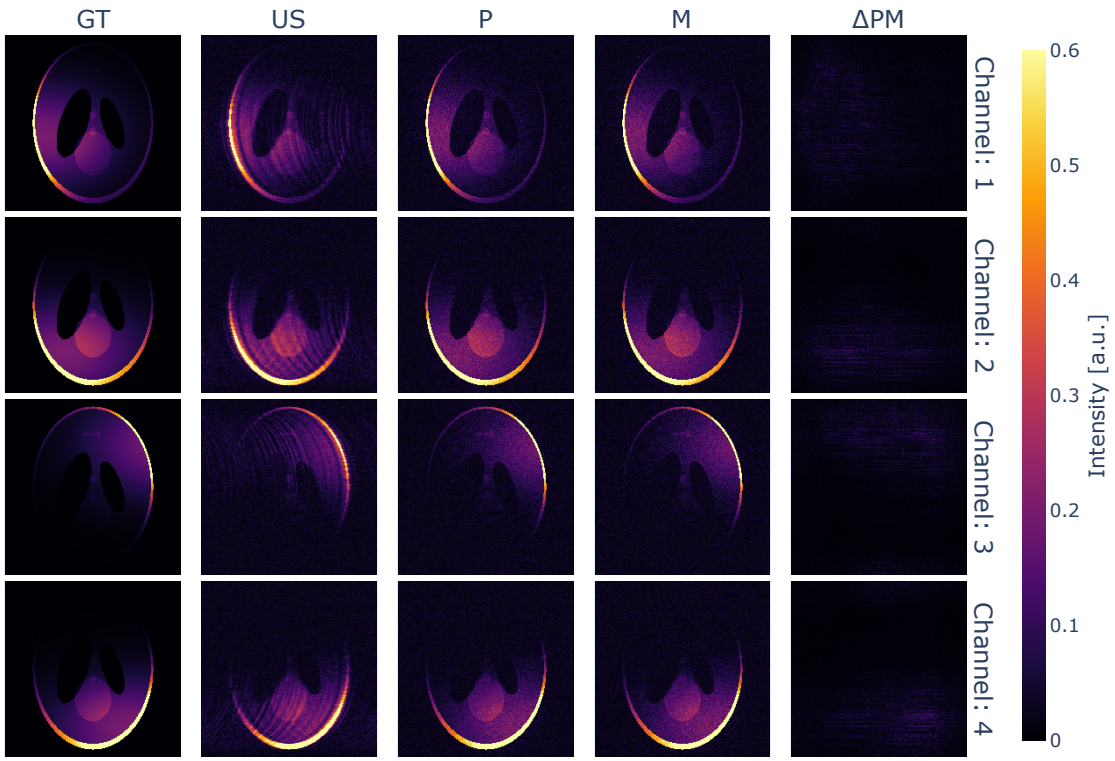

Figure 1: Example of a validation test between MLORAKS and PyLORAKS. The rows show four channels of the first echo of a 3-fold undersampled slice of a Shepp-Logan phantom ($200 \times 200 \times 8 \times 4$). The noise-free ground truth is provided in the first column (GT), while the undersampled and noise-corrupted input data is shown in the second column (US). After reconstruction, noisy images can be obtained by using PyLORAKS (P, third column) or MLORAKS (M, fourth column) joint-reconstruction with aligned algorithm parameters, which show a high level of agreement. The last column (ΔPM) shows the difference (P - M) which was multiplied by a factor of 1000 for visualisation purposes.

parametrised by θ, as an estimator of $\boldsymbol{k}_{\text{true}}$ given $\boldsymbol{k}_{\text{acq}}$, following the notation used in Ilicak et al. The SURE expression for a linear denoiser can be derived:[3]

$$\mathbb{E}\left\{\|\boldsymbol{P}_r(\boldsymbol{k}_{\text{acq}}) - \boldsymbol{k}_{\text{true}}\|_2^2\right\} = \mathbb{E}\left\{\text{SURE}_{\boldsymbol{P}_r}(\boldsymbol{k}_{\text{acq}})\right\} \ , \tag{1}$$

with

$$\text{SURE}_{\boldsymbol{P}_r}(\boldsymbol{k}_{\text{acq}}) = c + \|\boldsymbol{P}_r(\boldsymbol{k}_{\text{acq}}) - \boldsymbol{k}_{\text{acq}}\|_2^2 + 2\sigma^2 div(\boldsymbol{P}_r(\boldsymbol{k}_{\text{acq}})) \ , \tag{2}$$

with c being a constant independent of r and $\boldsymbol{k}_{\text{acq}}$ and σ is the noise variance. The latter can be estimated in different ways. In our case the data is pre-whitened, and noise prescans are available yielding straight forward extraction of σ.

We note that the independent LORAKS constraint ($J_r(\boldsymbol{P}(\boldsymbol{k})$ in Equation 1 of the main manuscript) can be seen as such a denoising operator when we set

$$\boldsymbol{P}_r = \boldsymbol{P}_S^{\star}\boldsymbol{P}_{\hat{S}_r}\boldsymbol{k}_{ac} \ , \tag{3}$$

with $\boldsymbol{P}_S$ being the LORAKS matrix operator for the S-matrix formalism, $\boldsymbol{P}_S^{\star}$ is its adjoint. $\hat{S}_r$ is the optimal rank-r approximation of the LORAKS S-matrix, i.e.

$$\hat{S}_r = U\Sigma_{\leq r,\leq r}V^H \ , \tag{4}$$

where all entries in Σ with row and column indices bigger than r have been replaced by 0, and consequently, $\boldsymbol{P}_{\hat{S}_r}$ is the operator creating this optimal rank-r matrix, by singular value thresholding. As prior work suggested, using only AC data achieves an optimum close to the true data optimum.[3] This is reasonable in the context of LORAKS, besides computationally more efficient, SURE yields an estimate using only acquired data, and the LORAKS matrix operator can be formed with complete neighbourhoods. However, the subsampling differences evaluated in the approach shown in this study are not recovered with this method as this yields identical parameter r estimates for identical AC regions.

We can find the divergence of the operator using PyLORAKS automatic gradient computation library combined with a Hutchinson's trace estimation.[4,5] The joint-reconstruction matrix size was kept fixed ($m_b = 3200$) to compare to the approach presented in our study. The optimal rank parameter was found using $\hat{r} = \min_r \mathrm{SURE}_r(\boldsymbol{k}_{\mathrm{acq}})$. We used the same input data and two loops of pointwise calculations varying $r = [100, \ldots, 300]$ in steps of 20 to yield $\hat{r}_o$, before using $r = [r_o - 20, \ldots, r_o + 20]$ in steps of 1 to find $\hat{r}$, taking ~ 45 min of computation time using PyLORAKS GPU capacities.

References

1. T. H. Kim and J. Haldar. *LORAKS 2.1: Implementation and Examples*. Last Accessed: 2025-07-18.
2. E. Ilicak, E. U. Saritas, and T. Çukur. "Automated Parameter Selection for Accelerated MRI Reconstruction via Low-Rank Modeling of Local k-Space Neighborhoods". In: *Zeitschrift für Medizinische Physik* 33.2 (2023), pp. 203–219. ISSN: 0939-3889. DOI: 10.1016/j.zemedi.2022.02.002.
3. S. Iyer, F. Ong, K. Setsompop, M. Doneva, and M. Lustig. "SURE-based automatic parameter selection for ESPIRiT calibration". In: *Magnetic Resonance in Medicine* 84.6 (2020), pp. 3423–3437. ISSN: 1522-2594. DOI: 10.1002/mrm.28386.
4. M. Hutchinson. "A Stochastic Estimator of the Trace of the Influence Matrix for Laplacian Smoothing Splines". In: *Communications in Statistics - Simulation and Computation* 18.3 (1989), pp. 1059–1076. ISSN: 1532-4141. DOI: 10.1080/03610918908812806.
5. M. Skorski. "Modern Analysis of Hutchinson's Trace Estimator". In: *2021 55th Annual Conference on Information Sciences and Systems (CISS)*. IEEE, 2021, pp. 1–5. DOI: 10.1109/ciss50987.2021.9400306.